A Remote Triggered Compound Parabolic Collector for Thermal Engineering Studies

https://doi.org/10.3991/ijet.v17i18.32155

Joshua D Freeman(✉), Umesh Mohankumar, Krishnashree Achuthan
Amrita Vishwa Vidyapeetham, Amritapuri Campus, Kollam, Kerala, India
joshdfreeman@am.amrita.edu

Abstract—Solar thermal energy systems are one of the most cost-effective renewable energy systems in use today. Engineering students study the design of these systems with the goal of learning how to design similar systems and perform research on improving the heating efficiency and overall operations. This paper elaborates on the design, construction, testing, and validation of a solar thermal system as a remote, open instrumentation lab, using two Compound Parabolic Collector (CPC) evacuated tube collectors with separate heating media. The lab allows for comparing heat transfer rates and collector efficiencies simultaneously for two fluids that have different thermal capacities. The heat patterns could be viewed using thermal cameras to analyze the CPC design. The unique feature of the system is its facility to control the lab remotely, as the setup is interfaced with instrumentation on a web server, thereby allowing students from geographically distant areas to access and perform experiments on the CPCs. A cumbersome lab with expensive hardware and outdoor requirements is thus made easy to perform and learn from via remote access. This remote methodology and hardware and IT architectures are especially pertinent and relevant in the blended and remote learning scenarios made common by the pandemic.

Keywords—solar thermal, compound parabolic collector, evacuated tube collector, remote triggered, virtual lab

1 Introduction

Solar thermal energy is a rapidly growing energy technology that finds application all over the world. One of the primary benefits of solar thermal energy is that it can be a very low cost and sustainable way of producing heat, requiring no fuel beyond natural sunlight, and producing no emissions in operation.

Concentrating solar thermal energy systems, are used to provide high quality process heat and usable steam for a variety of industrial processes, including commercial scale electricity generation, participating in combined heat and power (CHP) systems providing climate control and electricity for larger commercial buildings, commercial scale cooking, food drying, sterilizing and pasteurizing systems for agriculture, chemical process industries, desalination systems, and high temperature materials research,

among many others [1, 2]. Non-concentrating solar thermal systems are used to provide hot water for bathing and cleaning, and to heat swimming pool water, significantly extending the pool's usable season in many parts of the world, among other uses.

The compound parabolic collector (CPC) used consists of an absorber tube covered with an evacuated glass tube and placed above a highly reflecting external reflector that provides mild concentration [1]. The CPC absorbs incident solar radiation, converting it to heat and transferring it to a heat transfer fluid (HTF), often water or an oil.

Even small solar thermal systems require significant space, ranging from rooftop units a couple of square meters in size up to large commercial installations. All solar thermal systems require access to the sun, a significant surface area and materials to convert sunlight into heat, plumbing to the heat consumer, and often pumping systems. As such, the large area requirements of solar thermal energy systems do not lend themselves well to easy access for studying and conducting experiments on.

The objective of this work was to create a solar thermal open instrumentation lab using CPC collectors, which allows a variety of experiments to be conducted, facilitating remote learning, testing and analysis of solar thermal concepts and theory, using actual hardware. This open instrumentation lab has been created to allow people from all walks of life, in all parts of the world, to be able to study complex solar thermal engineering processes, theory and application, on actual lab equipment that they might not be able to otherwise access. This has become especially important and necessary during the pandemic.

This work was done as a part of an initiative to build online, virtual laboratories, VALUE @Amrita, at Amrita Vishwa Vidyapeetham (Amrita University) [3, 4]. The virtual, remote triggered laboratories give teachers an additional teaching aid to the conventional laboratories, provide remote access to large and expensive laboratory hardware, and to help students understand the theory by experimenting multiple times at their convenience.

2 Background study

Numerous works highlight the potential and capability of remote learning systems in engineering education, [5, 6]. Several papers also focused on what did not work during the recent pandemic and how the situation could be remedied [7, 8].

Relevant solar thermal energy engineering topics have been covered in innumerable publications. While the content of these papers is of great use to engineering students, the vast majority of these are not focused on high quality engineering education.

For example, the collector efficiency of a compound parabolic collector for different temperature and volumetric flow range was characterized experimentally in [9]. To calculate the thermal efficiency of the system, physical values are measured using a flow meter, a thermocouple and a pyranometer. The temperature at the inlet and outlet of the collector and its receiver were measured using thermocouple temperature sensors and acquired using DAQ devices into the LabVIEW software. However, in contrast to the work described in this paper, the experiment in [9] was a one-time test and was not hosted online for engineering students to repeat. In [10], remote monitoring and testing of a solar heater has been implemented in order to test a solar boiler for its efficiency

and look for previous results from a saved database. However, this setup is strictly industrial and is not geared towards repeat and broad educational use.

Thermal efficiency of different operating fluids can be compared using any solar thermal equipment. While experiments of this type could yield interesting results for solar engineering students and thermal engineering students, normal laboratory setups could be very complicated and difficult to utilize even in person and nearly impossible to learn from remotely. For example, the density, dynamic viscosity, specific heat capacity, thermal efficiency and thermal conductivity of different operating fluids are compared for research in [11]. In the work highlighted in this paper, the thermal properties and impacts of two different operating fluids can be compared and explored further, without having to acquire additional experimental setups.

In an experimental analysis by Swain et al. [12], a solar water heater uses a flat plate collector. The graph of mass flow rate vs. efficiency is plotted manually where a graduated beaker is used for flow measurement. In another work [13], a phase change material is used for heat retention and efficiency is calculated for different flow rates. These types of experiments are performed much more easily in the setup proposed here.

In the work by Motahhir et al., a solar tracker test bench [14] is developed for students to learn about the efficiency of PV panels, where a fixed axis PV panel and dual axis solar tracker working can be compared and analyzed with data from excel spreadsheets and graphs can be plotted. While the remote educational methodology is similar to the work in this paper, it is for studying solar photovoltaic systems, which are very different and vastly simpler than the solar thermal system incorporated here.

Finally, mathematical modeling is the theoretical solution for evaluating the thermal performance considering different parameters such as flow rate, velocity of flow, collector length, heat transfer media and assessing stored thermal energy [15, 16, 17]. Mathematical modelling, however, rarely captures all the physical phenomenon and interactions occurring in an actual hardware-based system such as shown here.

3 Methods and procedures

3.1 System description

The compound parabolic collector (CPC) used in this experiment is a flat plate collector composed of a number of evacuated glass tubes, each placed above a highly reflecting external reflector [18]. It was designed by the Fraunhofer Institute in Germany with the technology licensed for manufacturing by Ritter-Energie, GmbH, Germany. It is very efficient and is one of the few passive solar collectors that can make steam (albeit low temp), due to the combined effect of the CPC geometry and vacuum collector tubes.

In this work, two identical, remotely controlled evacuated tube compound parabolic collectors are connected in an experimental setup, with different heating media in each; namely, water and a petroleum (oil) based thermic fluid was used (Hytherm 600 [19]). The control and data acquisition programs were developed using the LabVIEW Virtual Instrumentation platform. Users can access and perform the experiments in real time from anywhere, using the internet. A scheduler prevents multiple users from attempting

to perform experiments at the same time, and allows experiments to be scheduled ahead of time, at the user's convenience.

In the experiments, the flow rate can be controlled remotely, and the inlet and outlet temperatures can be remotely measured at the same time. The experiment visualizer has an interface to a horizontal pyranometer experiment setup, whereby the Global Horizontal Irradiance (GHI) during the experiment can be measured and the thermal efficiency calculated [20].

These parabolic collector systems are installed on the rooftop terrace of an Amrita University, Amritapuri campus building, as shown in Figures 1 and 2.

Fig. 1. Experimental setup of compound parabolic collector with water

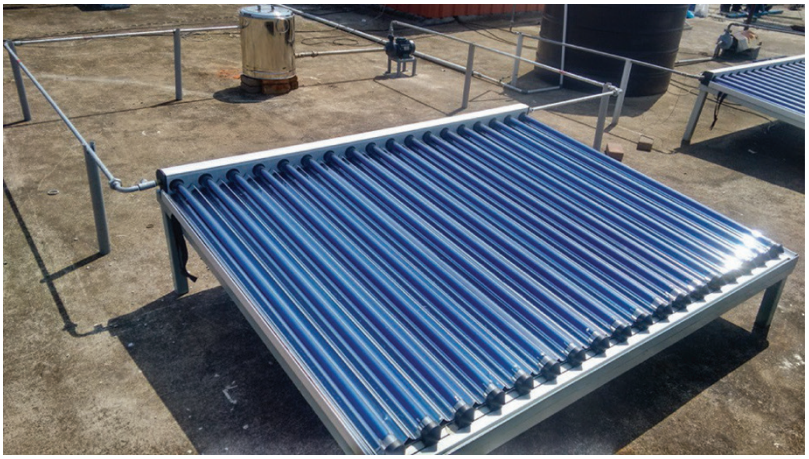

Fig. 2. Experimental setup of compound parabolic collector with oil

The setup consists of:

1. Three phase alternating current motor
2. Variable Frequency Drive (VFD)
3. Flowmeter
4. Compound Parabolic Collector (CPC)
5. Temperature measurement – Resistance Temperature Detector (RTD)
6. Data Acquisition Device (DAQ)
7. LabVIEW control server

The block diagram of the remote triggered CPC setup is shown in Figure 3.

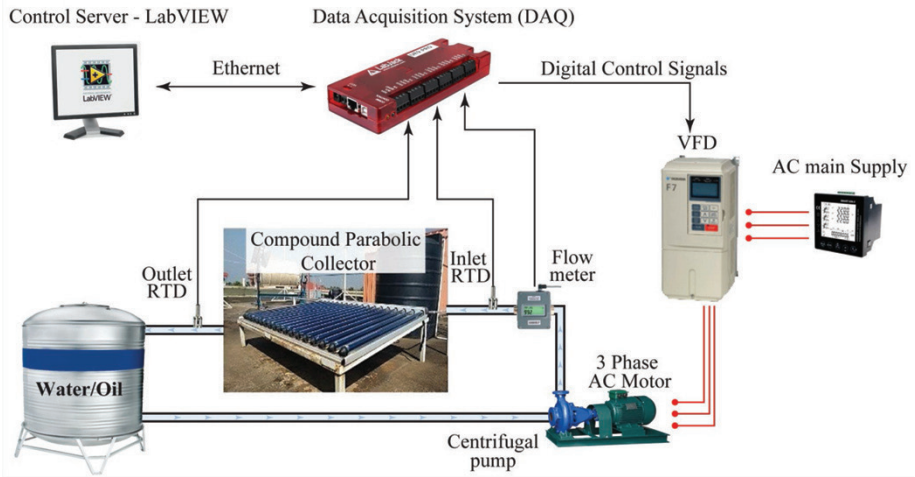

Fig. 3. Block diagram

Pumping mechanism. The flow rate of the working fluid is controlled using the VFD and motor/pump. The motor used is a 415V, 50Hz, 5A, three phase induction motor with speed controlled by a Yaskawa Varispeed F7 AC motor speed controller [21]. The speed of the motor is controlled by setting the appropriate control method and adjusting the frequency input to the VFD. Adjusting the drive output frequency will adjust the motor rpm. The three phase motor pumps the working fluid from the storage tank to the CPC according to the flow rate set by the user on the experiment webpage.

Temperature measurement. The collector inlet and outlet temperatures are monitored using RTDs. A three-wire PT-100 RTD [22] module is interfaced with the RTD data acquisition module [23]. A permanent IP address is provided to the RTD DAQ module which interfaces the module to the remote LabVIEW control server over local Ethernet.

Flowmeter. A flow meter installed in the collector inlet gives a voltage output of between 0–10 V, corresponding to the flow rate of the working fluid. The analog input terminal of the DAQ device captures the output voltage of the flow meter. As the analog input range of the DAQ is 5V, the output voltage from the flow meter is

reduced to 0–5V from 0–10V using a voltage divider circuit. Thus, the actual flow rate commanded by the user can be verified against the measured flow rate. The voltage corresponding to the flow rate is then converted into lpm (liter per minute) in in the LabVIEW control program.

Compound parabolic collector. The CPC used has 18 evacuated tubes connected in parallel, with a parabolic aluminum reflector behind each tube. The evacuated tubes consist of two concentric glass tubes, with the space between the tubes evacuated and hermetically sealed. A U-shaped copper tube is inserted into the inner glass tube. The inner glass tube is made with borosilicate and coated with an aluminum nitride heat absorber. The gross surface area of the CPC is 3.41 square meter, with an aperture area of 3.00 square meters. When light is concentrated on the collector, it is absorbed by the materials in the collector cavity and conducted to the working fluids. There are four heat transfer processes in the collector: solar radiation in the parabolic reflector, heat conduction on the collector glass surface and cavity walls, convection by the working fluids in the cavity and convective heat transfer between the cavity and air surrounding it.

Data acquisition device. The LabJack UE9 PRO DAQ module is used to interface the flow meter and VFD with the LabVIEW control server. As the analog output voltage range of the LabJack is 0–5V and the required analog input voltage range of the VFD is 0–10V, a LabJack "Tick" DAC (LJT DAC) module with an analog output voltage range of −10 to +10 volt is connected to the output pins of the DAQ module. The output of the LJT DAC is then connected to the analog input pin of the VFD to control the frequency, within the range of 0 to 50 Hz. A permanent IP address is assigned to the DAQ, which communicates with the remote LabVIEW control server over local Ethernet. As previously mentioned, the flow meter measures the flow rate and outputs, in terms of voltage, to the analog terminals of the DAQ; and, the DAQ outputs frequency-controlled voltage to the VFD.

LabVIEW control server. A desktop computer with LabVIEW software installed works as the control server. The control and data acquisition program were developed using the NI LabVIEW platform. The LabVIEW environment plays a key role in the communication between the server, DAQ and the remote hardware setup. Figure 4 shows a part of the LabVIEW code for control and data acquisition.

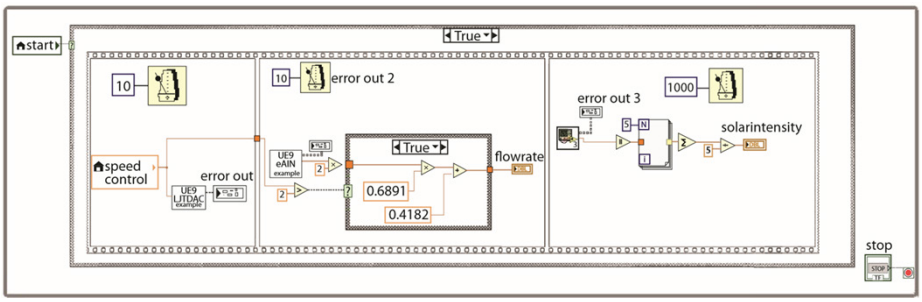

Fig. 4. LabVIEW code for control and data acquisition

Virtual lab collaborative accessibility platform (VLCAP). The VLCAP is a multi-tiered highly scalable architecture that supports collaborative development and deployment of remote systems [3, 4]. The data acquired through the DAQ is converted into graphs and streamed live onto the webpage, as can be seen in Figure 8. Realtime measured data is streamed in the station status window. A live video of the experiment is streamed on another window, which can be toggled to view the video from a thermal camera to analyze the heating pattern. Another window is interfaced to the pyranometer, also hosted as a related experiment at the same Amrita Virtual Labs website, where the live streaming of data is made available on the screen and can be downloaded for further analysis. The platform allows remote connectivity only if the remote hardware is not already being used by another user. If the equipment is busy, a 'remote machine not responding' message is displayed, and the user is given an option to schedule the experiment at a later time. The scheduling feature is also handled by the VLCAP. Hardware is protected from unauthorized access using Kerberos, a secure token authentication protocol [3]. The experiment is set for a 15-minute duration and can be adjusted by an administrator.

3.2 Architecture of the remote triggered laboratory

The architecture of the remote triggered lab is shown in Figure 5. The user's control input signals from the web-based Graphical User Interface (GUI) are transmitted to the Virtual Lab web server over HTTP, and then transmitted to the LabVIEW control server which is interfaced with the data acquisition hardware. The control signals interact with the experiment hardware setup to execute the LabVIEW code according to the flow rate selected by the user. Frequency signals corresponding to the flow rate are sent to the VFD which drives the three-phase motor to pump the working fluid. The flow meter at the inlet of the CPC measures the rate at which the working fluid is flowing into the CPC. Inlet and outlet RTDs [24] measure, respectively, the inlet and outlet temperatures and send the data to the RTD DAQ [25].

The global horizontal irradiance (GHI) value is acquired using an unshaded, horizontally mounted pyranometer [20, 21, 22, 23, 24]. The irradiance data is displayed in the web-based GUI, as can be observed in Figure 8. The inlet and outlet temperature and flowrate data are acquired by the data acquisition hardware and its control software over local Ethernet, sent to the web server and made available to the user on the GUI. A thermal camera is used to capture the temperature gradients and is streamed on the GUI, as in Figure 7. Measured data values, control input signals from the user end, thermal images and videos are all transmitted in real time, giving the user real time feedback and control over the remote system.

A key feature of this overall IT and experiment architecture is that it only requires the installation of a single Labview license on a central server, uses a standard internet browser webpage for the GUI, and requires no downloads or admin privileges at the client end, making the experiments cloud-based, easy to use, and free for the user.

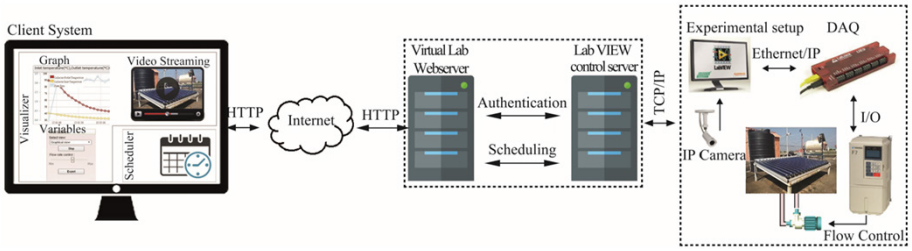

Fig. 5. Architecture

3.3 Accessing the lab

The lab was continuously hosted on the Amrita Virtual Labs website from 2011 through 2019. The process for accessing the lab was for users to create and use a free log-in on to the virtual lab website (www.vlab.amrita.edu) and select 'Solar Energy Labs' under the 'Mechanical Engineering' section and then select the 'External Compound Parabolic Collector – Water' or the 'External Compound Parabolic Collector – Oil' experiment links, to start the appropriate CPC experiment. After selecting the experiment, users are advised to go through the 'Theory', 'Procedure' and 'Self Evaluation' tabs, as shown in Figure 6, before performing the remote trigger (RT) experiment. The 'Theory' section gives some background information about the flat plate collectors, evacuated tube collectors and their working. The 'Procedure' tab provides step by step instructions on how to perform the experiment. The 'Self Evaluation' tab has a set of questions to check if the user has sufficient knowledge about the experiment and GUI procedure before performing the experiment. The 'Assignment' tab has follow-up questions to ensure that the user has gained proper learning from the experiment. Users can provide 'Feedback' on the effectiveness of the virtual lab experiment. Finally, the 'Dataset' tab provides sample data and graphs to help users learn the calculations and theory when the experiment is unavailable.

The GUI of the experiment is divided into sub-windows, as can be observed in Figures 8 and 9. The sub-window on the top left displays the graphical plots obtained for inlet temperature, outlet temperature, flow rate and GHI vs time. Using the 'Select view' drop down control, the user can select the actual live streaming video of the experiment setup on the 'image view' window or the live video from the thermal camera. This streaming video provides a real time feel of the actual experiment.

The user starts the experiment by clicking on the 'Start' button. User adjustable buttons and sliders under the 'Variables' section at the top-right of the GUI allow the user to remotely control the experiment. The flow rate of the working fluid can be controlled in real time by adjusting the 'Flow rate control' slider. By selecting different flow rates, the users can observe the variations in the heat transfer rate. The real-time data stream is displayed in the 'station status' section, and each value is plotted on the graph. The data can be downloaded as a CSV file using the 'Export' button for further analysis.

From the results shown in the GUI (Figure 9), the user can validate what they learned from the theory. They also have a provision to manually perform thermal efficiency calculations, by downloading the real time experimental data, using the 'Export' button. The difference in efficiency between water and oil media can be compared along with their temperature variations.

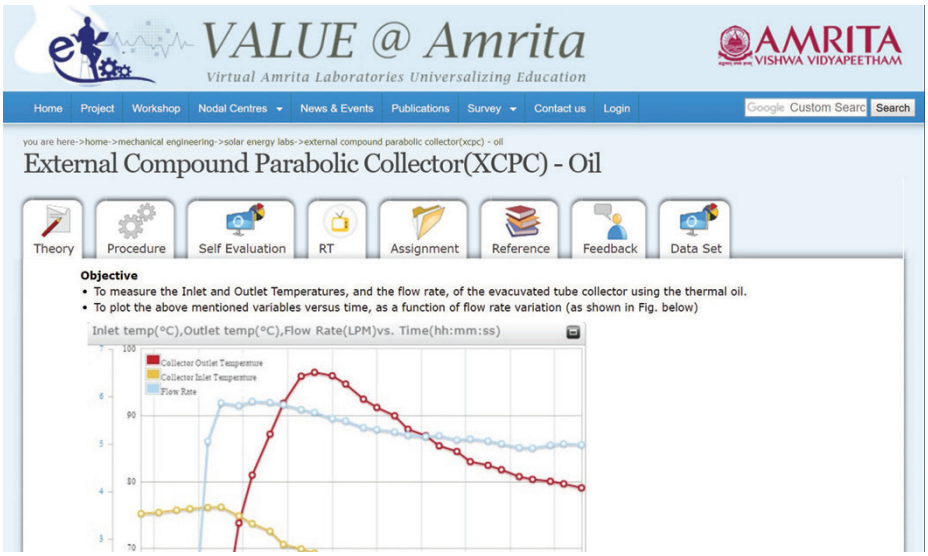

Fig. 6. CPC experiment page

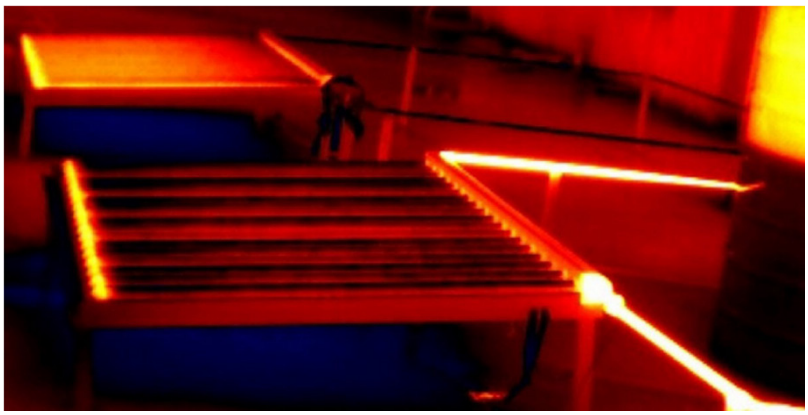

Fig. 7. Thermal camera view of the water and oil-based CPCs

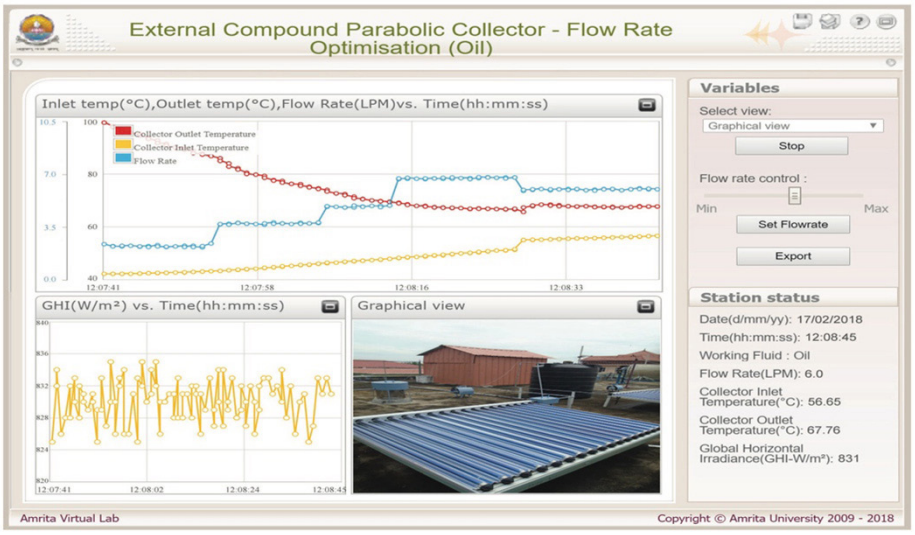

Fig. 8. GUI for the external compound parabolic collector

4 Results

Data from the CPC flat plate collector experiment is shown in Figure 9, with data collected at approximately noon on May 31st, 2015. The weather on coastal Kerala, India, at this time of year is before the 1st monsoon, with zero precipitation and very constant temperatures. This data was analyzed to determine the fit of the predicted output temperatures to the observed readings.

The data can be broken into several sections, as indicated by the vertical bars on Figure 9 and the associated lettering at the top of each section.

(A) Data in this section, from the beginning of the plot up until the first vertical marker line, can be disregarded. The pump speed is at zero liters/min (lpm), the collector is stagnated, and the experiment process has not yet started.
(B) Data in this section can also be disregarded. The pump has now been turned on, rising to its maximum speed of 5 lpm, and is flushing the stagnated water past the output sensor, located a few inches outside the CPC, causing the high outlet temperatures seen as the hot water flows out through the outlet and into the 5000-liter holding tank, also shown in Figure 9.
(C) The temperature has stabilized with a constant flow rate of 5.0 lpm in this section. Our analysis will start with this section.
(D) The flow rate is reduced to the next set point of 3.7 lpm and we see an associated, expected rising in outlet temperature.
(E) The outlet temperature has stabilized for the flow rate of 3.7 lpm.
(F) The flow rate is again reduced to the next set point of 2.5 lpm and we see the expected rising in outlet temperature.

(G) The outlet temperature again stabilizes for 2.5 lpm.
(H) The flow rate is again reduced to the next set point of 1.0 lpm.
(I) The outlet temperature stabilized for 1.0 lpm.
(J) Data in this section can be disregarded. The pump is turned off and the temperature at the outlet remains stable from the previous pump speed setting.

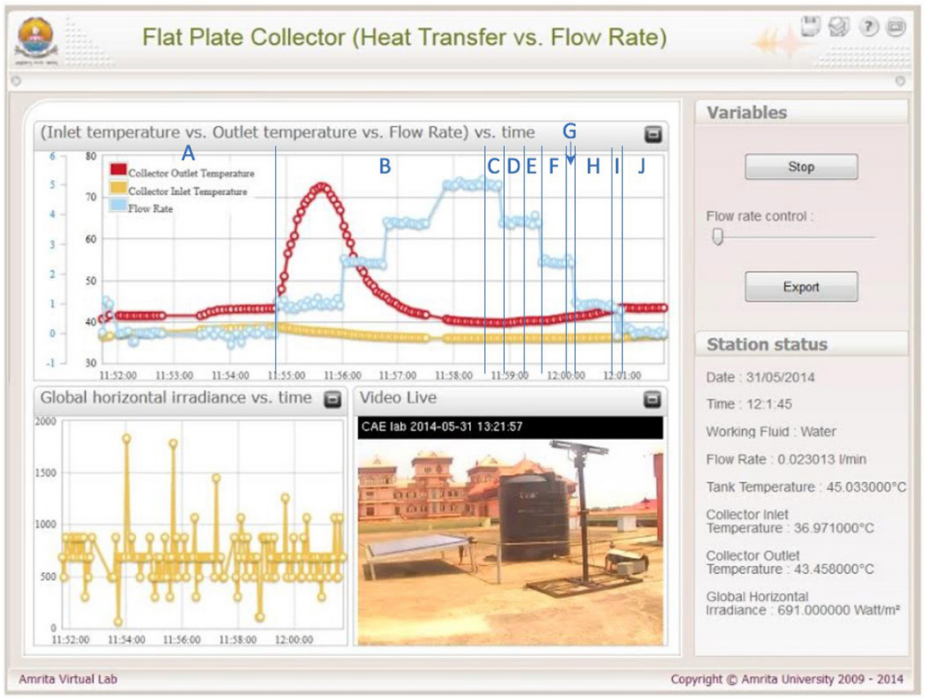

Fig. 9. Experimental data being analyzed

The above data was analyzed in order to validate the operation and theory of the system. Successful validation would involve being able to closely predict the output temperature of the system for a given incident solar irradiation, flow rate, and thermal transfer fluid characteristics.

The key collector parameters are taken from the CPC datasheet [18] and are given in Table 1. The thermal transfer fluid used in the experiment was water, which has a specific heat index of 4.186 kJ/(kg·C°)), which converts to 1.163 Wh/(kg·C°). The solar irradiation, as measured by the pyranometer, averaged 691 W/m^2.

The key parameters of the CPC are found in the datasheet [20] and listed in Table 1.

Table 1. Physical properties of the collector

Symbol	Property	Value
A_C	Aperture area of the collector	3.0 m^2
η_0	Zero loss efficiency	0.644%
η_C	Collector efficiency	0.61%
a_1	First order heat transfer coefficient	0.75
a_2	Second order heat transfer coefficient	0.005
IAM	Installation Angle Modifier	1

5 Analysis

The following derivations of the relationship between the outlet temperature, solar irradiation, flow rate and properties of thermal transfer fluid, are founded on Chapter 3 of [25] which describes the general theory behind flat plate collectors. This theory also applies to compound parabolic collectors, CPC, which is essentially a flat plate collector with low thermal losses due to the vacuum tubes and high optical efficiency resulting from the compound parabolic reflector below each vacuum tube. This flat plate collector theory was extended by the authors to solve for additional results with higher accuracy that used more of the parameters provided in the CPC datasheet.

$\dot{Q}_{RC}$ describes the thermal losses of the collector and is given in (1). This ties the losses to the aperture area of the collector, A_C, the temperature of the collector, θ_C, the ambient temperature, θ_A, and the first and second order heat transfer coefficients, a_1 and a_2, respectively.

$$\begin{aligned}\dot{Q}_{RC} &= a_1 \cdot A_C \cdot (\theta_C - \theta_A) + a_2 \cdot A_C \cdot (\theta_C - \theta_A)^2 \\ &\approx a \cdot A_C \cdot (\theta_C - \theta_A)\end{aligned} \tag{1}$$

Equation (2) gives the collector efficiency, η_C, as the CPC collector's power output, $\dot{Q}_{out}$, divided by the product of the solar irradiation, E, and the area of the collector surface A_C. This is equal to the optical efficiency η_0 minus $\dot{Q}_{RC}$, the sum of the convection and radiation losses, divided by E times A_C.

$$\eta_C = \frac{\dot{Q}_{out}}{E \cdot A_C} = \eta_0 - \frac{\dot{Q}_{RC}}{E \cdot A_C} \tag{2}$$

Starting with (2) above, rearranging terms, and substituting for $\dot{Q}_{RC}$ from (1), we obtain (3):

$$\eta_C = \eta_0 - \frac{a_1 \cdot (\theta_C - \theta_A) + a_2 \cdot (\theta_C - \theta_A)^2}{E}. \tag{3}$$

From Table 1, a_2 is two orders of magnitude smaller than a_1, leading to the approximated, simplified form of η_C, given in the right half of (3).

Equation 4 gives the collector flow rate $\dot{m}$ as a function of the collector power output $\dot{Q}_{out}$, c, the heat capacity of the thermal transfer fluid, and $\Delta\theta_{HTF}$, the temperature difference of the thermal transfer fluid between the inlet and outlet.

$$\dot{m} = \frac{\dot{Q}_{out}}{c \cdot \Delta_{HTF}} \tag{4}$$

Solving (2) for $\dot{Q}_{out}$, then substituting (3) for η_C, the collector flow rate is then given by:

$$\dot{m} = \frac{\eta_0 \cdot E \cdot A_C - a_1 \cdot A_C \cdot (\theta_C - \theta_A) - a_2 \cdot A_C \cdot (\theta_C - \theta_A)^2}{c \cdot \Delta\theta_{HTF}}, \tag{5}$$

while the flow rate of the collector with respect to the aperture area of the collector, A_C, then becomes:

$$\begin{aligned} \dot{m}' = \frac{\dot{m}}{A_C} &= \frac{\eta_0 \cdot E - a_1 \cdot (\theta_C - \theta_A) - a_2 \cdot (\theta_C - \theta_A)^2}{c \cdot \Delta\theta_{HTF}} \\ &\approx \frac{\eta_0 \cdot E - a \cdot (\theta_C - \theta_A)}{c \cdot \Delta\theta_{HTF}}. \end{aligned} \tag{6}$$

Equations 7 and 8 give $\Delta\theta_{HTF}$ as the difference between $\theta_{C_{in}}$, the temperature of the fluid at the inlet of the collector, and $\theta_{C_{out}}$, the temperature of the fluid at the outlet of the collector, yielding θ_C as the temperature of the collector, given as the average of $\theta_{C_{in}}$ and $\theta_{C_{out}}$.

$$\Delta\theta_{HTF} = \theta_{C_{out}} - \theta_{C_{in}} \tag{7}$$

$$\theta_C = \frac{\theta_{C_{out}} + \theta_{C_{in}}}{2} \tag{8}$$

Substituting (7) and (8) into (6), gives (9), the temperature of the collector outlet, $\theta_{C_{out}}$, as a function of the collector inlet temperature, $\theta_{C_{in}}$, and other known terms.

$$\theta_{out} = \theta_{C_{out}} = \frac{\eta_0 \cdot E + \dot{m}' \cdot C \cdot \theta_{C_{in}} + a \cdot \left(\theta_A - \frac{1}{2}\theta_{C_{in}} \right)}{\dot{m}' \cdot C + \frac{1}{2}a} \tag{9}$$

The results of (9) are plotted in Figure 10 as θ_{out} (predicted by (9)), which is a good match with the measured temperature. When using (9), care must be taken to ensure that the various input parameters have been converted to the correct units, particularly, the flow rate, $\dot{m}'$, and the specific heat of the thermal transfer fluid, c.

An alternative method of solving for the predicted θ_{out} is presented next. Since the datasheet for the CPC collector gives the second order heat coefficient term, a_2, (6) was also solved without approximating the second order term, $a_2*(\theta_C - \theta_A)$, to be zero. Through basic algebra and separating the known terms from the unknowns, we obtain a quadratic polynomial with θ_{out} as the unknown variable:

$$A \cdot (\theta_{out})^2 + B \cdot (\theta_{out}) + C = 0 \tag{10}$$

where, A, B, and C are composed of known quantities:

$$A = \frac{a_2}{4},$$

$$B = \frac{\dot{m} \cdot C}{A_C} + \frac{a_1}{2} - (a_2 \cdot \theta_A) + (2 \cdot a_2 \cdot \theta_{in}), \quad and$$

$$C = (\eta_0 \cdot E) + (a_1 \cdot \theta_A) - (a_2 \cdot \theta_A^2) + (a_2 \cdot \theta_A \cdot \theta_{in}) + \frac{\dot{m} \cdot d \cdot \theta_{in}}{A_c} - \frac{a_1 \cdot \theta_{in}}{2} - (a_2 \cdot \theta_{in}^2)$$

Solving the quadratic equation yields one real root, providing results that match decently over a large part of the plot with the measured values of θ_{out}, shown in Figure 10.

The data and implementation of (9) and (10) are shown in Figure 10 and Table 2.

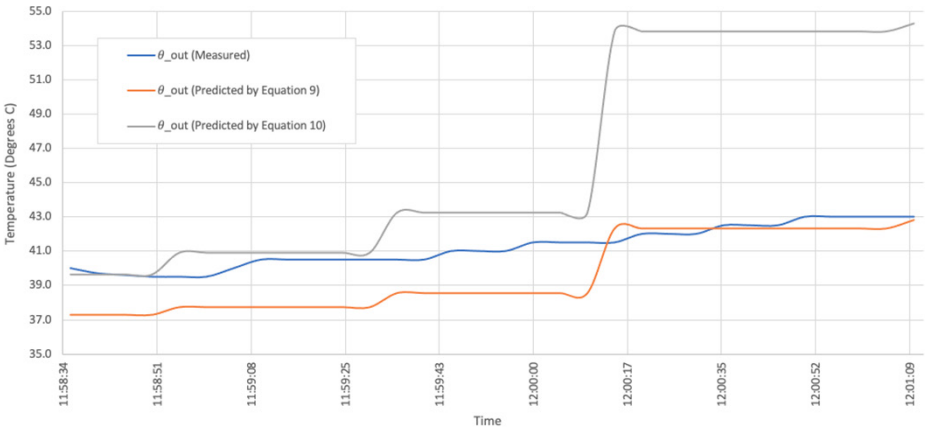

Fig. 10. Plot of the predicted θ_{out} values vs. the measured θ_{out}

6 Discussion

As can be seen in Figure 10, the first method of predicting θ_{out}, using (9), yields results which are overall close to the measured θ_{out} temperatures, especially at the lower flow rates towards the end of the experiment. The second method of predicting θ_{out}, using the quadratic roots, gives temperatures that are closer to the measured θ_{out} at high

flow rates at the beginning of the analysis and significantly far off at the lower flow rates. Overall, the two methods used for prediction indicates that the experiment is performing roughly as predicted by the theory.

One source of error is the unknown starting temperature of the collector itself, due to its previously stagnated condition, and exactly how the collector temperature decreases as the thermal fluid flows at various flow rates. This can account for some of the differences between the two predicted methods for θ_{out} and the measured θ_{out} values.

7 Conclusion

Two solar thermal Compound Parabolic Collectors, one with water as the thermic fluid and one with Hytherm 600, have been setup as open instrumentation labs. These labs have been successfully designed, interfaced, installed, tested, and validated. The CPC open access lab was connected to and remotely operated over the internet from anywhere in the world, without downloading or purchasing software licenses. Users could adjust the flow rates and measure the inlet and outlet temperatures of the CPCs. A simultaneous solar insolation data stream from a pyranometer is also made available on the GUI, with the corresponding plots.

Table 2. Calculations data and implementation

Chart Label	Time (hr:min:sec)	E (W/m2) (averaged)	θ_in (C)	$\dot{m}$ (lpm)	θ_out (Measured)	θ_out (Predicted by Equation 9)	A	B	C	θ_out (Predicted by Equation 10)
C - Stable temp @ 5.0 lpm	11:58:35	691	36.0	5.0	40.0	37.3	0.001	116.9	-4636	39.7
	11:58:40	691	36.0	5.0	39.7	37.3	0.001	116.9	-4636	39.7
	11:58:45	691	36.0	5.0	39.6	37.3	0.001	116.9	-4636	39.7
	11:58:50	691	36.0	5.0	39.5	37.3	0.001	116.9	-4636	39.7
D - Rising temp @ 3.7 lpm	11:58:55	691	36.0	3.7	39.5	37.7	0.001	86.63	-3548	40.9
	11:59:00	691	36.0	3.7	39.5	37.7	0.001	86.63	-3548	40.9
	11:59:05	691	36.0	3.7	40.0	37.7	0.001	86.63	-3548	40.9
	11:59:10	691	36.0	3.7	40.5	37.7	0.001	86.63	-3548	40.9
E - Stable temp @ 3.7 lpm	11:59:15	691	36.0	3.7	40.5	37.7	0.001	86.63	-3548	40.9
	11:59:20	691	36.0	3.7	40.5	37.7	0.001	86.63	-3548	40.9
	11:59:25	691	36.0	3.7	40.5	37.7	0.001	86.63	-3548	40.9
	11:59:30	691	36.0	3.7	40.5	37.7	0.001	86.63	-3548	40.9
F - Rising temp @ 2.5 lpm	11:59:35	691	36.0	2.5	40.5	38.5	0.001	58.72	-2543	43.3
	11:59:40	691	36.0	2.5	40.5	38.5	0.001	58.72	-2543	43.3
	11:59:45	691	36.0	2.5	41.0	38.5	0.001	58.72	-2543	43.3
	11:59:50	691	36.0	2.5	41.0	38.5	0.001	58.72	-2543	43.3
	11:59:55	691	36.0	2.5	41.0	38.5	0.001	58.72	-2543	43.3
G - Stable temp @ 2.5	12:00:00	691	36.0	2.5	41.5	38.5	0.001	58.72	-2543	43.3
	12:00:05	691	36.0	2.5	41.5	38.5	0.001	58.72	-2543	43.3
H - Rising temp @ 1.0 lpm	12:00:10	691	36.0	2.5	41.5	38.5	0.001	58.72	-2543	43.3
	12:00:15	691	36.0	1.0	41.5	42.3	0.001	23.83	-1287	53.9
	12:00:20	691	36.0	1.0	42.0	42.3	0.001	23.83	-1287	53.9
	12:00:25	691	36.0	1.0	42.0	42.3	0.001	23.83	-1287	53.9
	12:00:30	691	36.0	1.0	42.0	42.3	0.001	23.83	-1287	53.9
	12:00:35	691	36.0	1.0	42.5	42.3	0.001	23.83	-1287	53.9
	12:00:40	691	36.0	1.0	42.5	42.3	0.001	23.83	-1287	53.9
	12:00:45	691	36.0	1.0	42.5	42.3	0.001	23.83	-1287	53.9
I - Stable @ 1.0 lpm	12:00:50	691	36.0	1.0	43.0	42.3	0.001	23.83	-1287	53.9
	12:00:55	691	36.0	1.0	43.0	42.3	0.001	23.83	-1287	53.9
J - Stable @ 0.0 lpm	12:01:00	691	36.0	1.0	43.0	42.3	0.001	23.83	-1287	53.9
	12:01:05	691	36.0	1.0	43.0	42.3	0.001	23.83	-1287	53.9
	12:01:10	691	36.5	1.0	43.0	42.8	0.001	23.84	-1298	54.3

8 Acknowledgements

The authors acknowledge their sincere gratitude and thanks to Sri Mata Amritanandamayi Devi, Chancellor, Amrita University. They also wish to thank the Indian Government's Ministry of Human Resource Development (MHRD) for funding the Amrita Virtual Labs project. which hosts hundreds of experiments in Engineering, Physics, Chemistry, and Biotechnology. Mr. Saneesh P. Francis is hereby thanked for helping with the figures. Dr. Balakrishnan Shankar and the Department of Mechanical Engineering are acknowledged for helping with the mechanical assembly. We wish to thank the Amrita CREATE team for the development of the Virtual Lab Collaborative Accessibility Platform (VLCAP).

9 References

[1] M. Jradi, S. Riffat, "Medium temperature concentrators for solar thermal applications", International Journal of Low-Carbon Technologies 9 (2012) 214–224. https://doi.org/10.1093/ijlct/cts068

[2] S. A. Kalogirou, "Solar thermal collectors and applications", Progress in Energy and Combustion Science 30 (2004) 231–295. https://doi.org/10.1016/j.pecs.2004.02.001

[3] R. Raman, P. Nedungadi, K. Achuthan, S. Diwakar, "Integrating collaboration and accessibility for deploying virtual labs using VLCAP", International Transaction Journal of Engineering, Management, & Applied Sciences & Technologies 2 (2011) 547–560.

[4] K. Achuthan, K. Sreelatha, S. Surendran, S. Diwakar, P. Nedungadi, S. Humphreys, S. S. CO, Z. Pillai, R. Raman, A. Deepthi, et al., "The Value@ Amrita Virtual Labs project: using web technology to provide virtual laboratory access to students", in: 2011 IEEE Global Humanitarian Technology Conference, IEEE, pp. 117–121. https://doi.org/10.1109/GHTC.2011.79

[5] S. Seiler, R. Sell, D. Ptasik, "Embedded system and robotic education in a blended learning environment utilizing remote and virtual labs in the cloud, accompanies by 'Robotic Home-Lab Kit'", International Journal of Emerging Technologies in Learning 7(4) (2012) 26–33. https://doi.org/10.3991/ijet.v7i4.2245

[6] C. Leao, F. O. Soares, J. Machado, E. Seabra, H. Rodrigues, "Design and development of an industrial network laboratory", International Journal of Emerging Technologies in Learning 6(S1) (2011) 21–26. https://doi.org/10.3991/ijet.v6iS1.1615

[7] R. M. I. Khan, A. Ali, A. Alourani, "Investigating learners' experience of autonomous learning in E-learning context", International Journal of Emerging Technologies in Learning 17(8) (2022) 4–17. https://doi.org/10.3991/ijet.v17i08.29885

[8] M. A. Ali, N. Sahari, S. Fadzilah, Zainudin, "Identifying students' learning patterns in online learning environments: a literature review", International Journal of Emerging Technologies in Learning 17(8) (2022) 189–205. https://doi.org/10.3991/ijet.v17i08.29811

[9] A. Ciucci, "Experimental characterization of the efficiency of a compound parabolic solar collector" (2016).

[10] G. S. de Arregui, M. Plano, F. Lerro, L. Petrocelli, S. Marchisio, S. Concari, V. Scotta, "A mobile remote lab system to monitor in situ thermal solar installations", in: 2012 9th International Conference on Remote Engineering and Virtual Instrumentation (REV), IEEE, pp. 1–4. https://doi.org/10.1109/REV.2012.6293142

[11] E. Bellos, C. Tzivanidis, "Thermal analysis of parabolic trough collector operating with mono and hybrid nanofluids", Sustainable Energy Technologies and Assessments 26 (2018) 105–115. https://doi.org/10.1016/j.seta.2017.10.005
[12] B. Swain, S. A. Memon, A. M. Achari, "Parametric analysis of inclined flat plate collector: A review with case study", International Journal of Applied Engineering Research 14 (2019) 1658–1667.
[13] M. Al Imam, M. R. A. Beg, M. Rahman, "Experimental analysis on the photovoltaic-thermal solar collector with compound parabolic concentrator using phase change material-towards solar energy utilization", Journal of Engineering Science and Technology 13 (2018) 3964–3979.
[14] S. Motahhir, A. E. Hammoumi, A. E. Ghzizal, A. Derouich, "Open hardware/software test bench for solar tracker with virtual instrumentation", Sustainable Energy Technologies and Assessments 31 (2019) 9–16. https://doi.org/10.1016/j.seta.2018.11.003
[15] R. Tchinda, "Thermal behaviour of solar air heater with compound parabolic concentrator", Energy Conversion and Management 49 (2008) 529–540. https://doi.org/10.1016/j.enconman.2007.08.004
[16] F. Cavallaro, "Fuzzy topsis approach for assessing thermal energy storage in concentrated solar power (CSP) systems", Applied Energy 87 (2010) 496–503. https://doi.org/10.1016/j.apenergy.2009.07.009
[17] Z. Cheng, Y. He, J. Xiao, Y. Tao, R. Xu, "Three-dimensional numerical study of heat transfer characteristics in the receiver tube of parabolic trough solar collector", International Communications in Heat and Mass Transfer 37 (2010) 782–787. https://doi.org/10.1016/j.icheatmasstransfer.2010.05.002
[18] Ritter, CPC 18 OEM, ritter-energie.de/en/cpc-oem-evacuated-tube-collectors/, 2013.
[19] Hytherm 600, http://www.hplubricants.in/products/specialties/thermic-fluids/hytherm-500-and-600-thermic-fluid-oil, 2021. Accessed: 15 February 2021.
[20] J. D. Freeman, R. Kumar, K. Achuthan, "Solar monitoring system for measuring solar radiation intensity", 2019. US Patent 10,295,404.
[21] VFD F7, www.yaskawa.com/products/drives/industrial-ac-drives/general-purpose-drives/f7-drive, 2012.
[22] Four channel RTD input data acquisition module, http://www. omega.com/en-us/communication-and-connectivity/data-acquisition-modules/p/PT-104A-Series, 2012.
[23] Pt104a data sheet, www.omega.com/en-us/data-acquisition/data-acquisition-modules/p/PT-104A-DAQ-Module, 2012. Accessed: August 25, 2019.
[24] A. Varghese, A. M. Vasanthakumary, J. Freeman, K. Achuthan, "Remote triggered solar energy assessment using a pyrheliometer and a pyranometer", in: 2017 IEEE 6th International Conference on Renewable Energy Research and Applications (ICRERA), IEEE, pp. 115–120. https://doi.org/10.1109/ICRERA.2017.8191251
[25] V. Quaschning, Understanding Renewable Energy Systems, Earthscan, 2005.

10 Authors

Joshua D Freeman was the team leader for the Amrita Virtual Labs Mechanical Engineering projects and is currently working on his PhD from Amrita Vishwa Vidyapeetham, Amritapuri Campus, in the field of concentrating solar thermal energy and has bachelors and master's degrees from the US. He is employed in the US automotive industry in heavy-duty vehicle propulsion systems. Josh has deep experience with

various aspects of electrified vehicles including high voltage architectures, charging, energy storage systems and others.

Umesh Mohankumar received his master's degree in Power and Energy from Amrita Vishwa Vidyapeetham, Coimbatore Campus, in 2014. He worked as a Research Associate with the Virtual Labs project at Amrita Vishwa Vidyapeetham, Amritapuri Campus, before moving to work in the renewable energy industry. He is currently working in the field of design and installation of Solar PV systems in Dubai, UAE. His areas of interests include renewable energy and power systems.

Dr. Krishnashree Achuthan is the director of the Amrita Center for Cybersecurity Systems and Networks at the Amritapuri Campus of Amrita Vishwa Vidyapeetham and has been pioneering the design, development, and implementation of Virtual Labs for close to a decade. She has a PhD from the US. Her areas of interest include Internet and Communication, as well as Educational Technologies, amongst others.

Article submitted 2022-05-02. Resubmitted 2022-07-03. Final acceptance 2022-07-03. Final version published as submitted by the authors.